

Supporting Information

Polyoxometalate-based self-adhesive hydrogels with both proton conductive and photochromic functions

Shuping Xue, Ying Lu*, Jun Geng, Jingqi Yang, Maochun Zhu, Xue Bai, Shuxia Liu*

*Key Laboratory of Polyoxometalate and Reticular Material Chemistry of Ministry of Education,
College of Chemistry, Northeast Normal University, Changchun 130024, China.*

* Corresponding authors:

Ying Lu (E-mail: luy968@nenu.edu.cn)

Shuxia Liu (E-mail: liusx@nenu.edu.cn)

This Information includes:

Section 1. Experimental section

1.1 Characterization

The X-ray photoelectron spectroscopy (XPS) spectra were measured by USA-Thermo Fisher Scientific-ESCALAB 250Xi. The content of Mo element was performed by using a PLASMASPEC(I) ICP atomic emission spectrometer. Scanning electron microscopy (SEM) images were determined by ZEISS Gemini SEM 300 (Germany). Fourier transform infrared (FTIR) spectra were recorded on an Alpha Centauri spectrometer in the range of 4000-400 cm^{-1} . The mechanical properties of the samples were measured by a AILIGU electric tensile tester at room temperature under the strain rate of 96 mm min^{-1} . The length, width, and thickness of the sample were about 23 mm, 11 mm, and 1.7 mm.

1.2 Water retention test

The PHGMO-15% hydrogel and PHMo hydrogel were placed at the environment with the temperature of 25°C and ambient humidity(40% RH). The water retention ability of the hydrogels at different time were calculated by the following equation:

$$\text{Water retention (\%)} = \frac{m_t}{m_0} \times 100\%$$

where m_0 and m_t were the weight of hydrogel at time 0 and time t, respectively.

1.3 Proton conductivity measurement

The obtained hydrogels were cut into rectangular samples, sandwiched between two copper sheets, and then placed in a Memmert HCP108 constant temperature and humidity chamber. AC impedance testing was performed on a Solartron SI 1260 Impedance/Gain Phase Analyzer. The frequency range is 0.1 Hz to 1MHz at 50 mV amplitude voltage. Proton conductivity is calculated according to the following equation:

$$\sigma = \frac{l}{S \times R}$$

where σ is the proton conductivity, l and S are the thickness and area of the hydrogel sample to be tested, respectively, and R is the impedance measured by the analyzer.

1.4 Photochromic exhibition of hydrogels

A UV lamp ($\lambda_{\max} = 365 \text{ nm}$) was used to do direct visual colorimetric observation for hydrogels after they were exposed to UV light. The samples were placed 15 cm from the light source, and the average light intensity was $\sim 70 \text{ mW/cm}^2$. The fading experiment of the hydrogels was conducted in an air-filled sealed plastic bag. To keep the hydrogel samples from drying out during the experiment, two or three drops of water were introduced to the plastic bag.

1.5 Absorbance measurement

A UV-visible spectrophotometer (50 Conc) was used to measure the UV-vis absorbance spectra. The 800–200 nm scanning range was chosen. $24000 \text{ nm}\cdot\text{min}^{-1}$ was the scan speed. The thickness of samples was set at 1.7 mm, and every sample was secured on the sample rack.

1.6 Assembly and testing of the strain sensors

The strain sensor was assembled by fixing the two ends of PHGMO-15% on the skin surface with copper tape with wire. The electrochemical workstation CHI760E was used to test the current-time curve. The following formula was used to determine the relative resistance change of hydrogels:

$$\frac{\Delta R}{R_0} = \frac{R - R_0}{R_0}$$

where $R_0 (\Omega)$ is the initial resistance and $R (\Omega)$ is the real-time resistance.

Section 2: Supplementary Figures

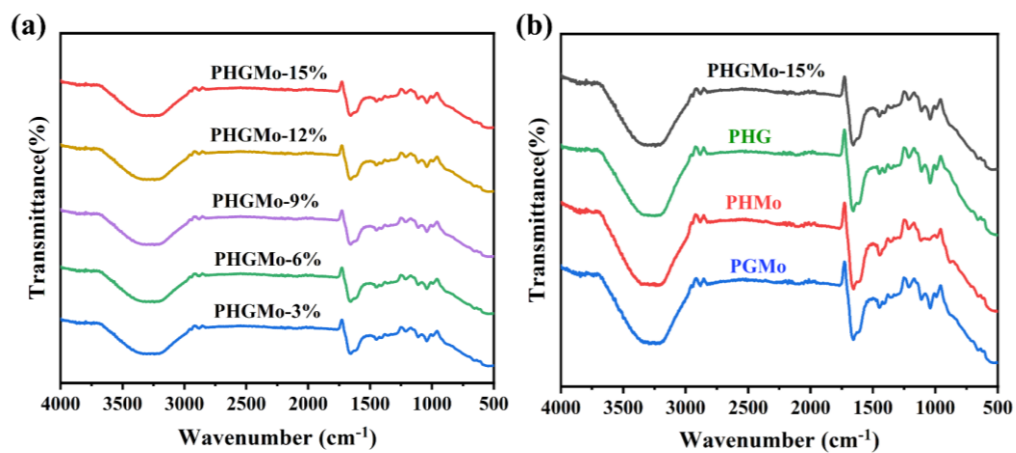


Figure S1. (a) Comparison of the FTIR spectra of PHGMo-x% hydrogels; (b) Comparison of the FTIR spectra of PHGMo-15%, PHG, PHMo and PGMo.

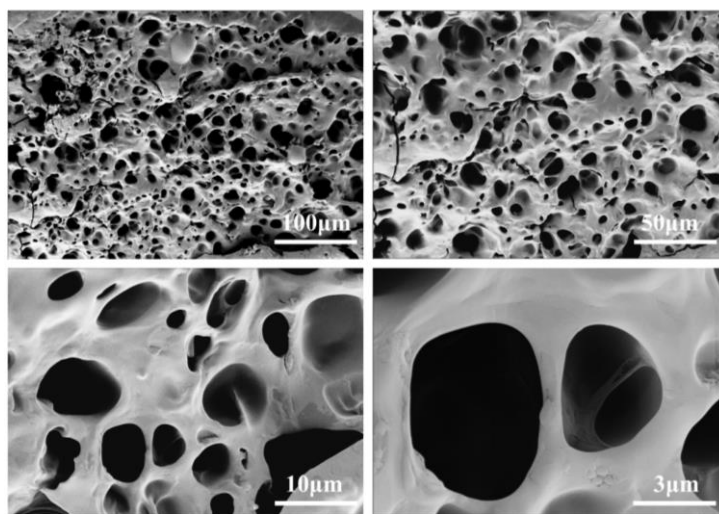


Figure S2. SEM images of PHGMo-15% hydrogel.

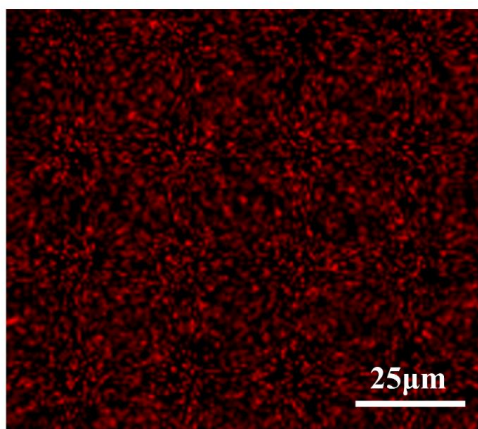


Figure S3. EDS element mapping of PHGMo-15% hydrogel (Mo).

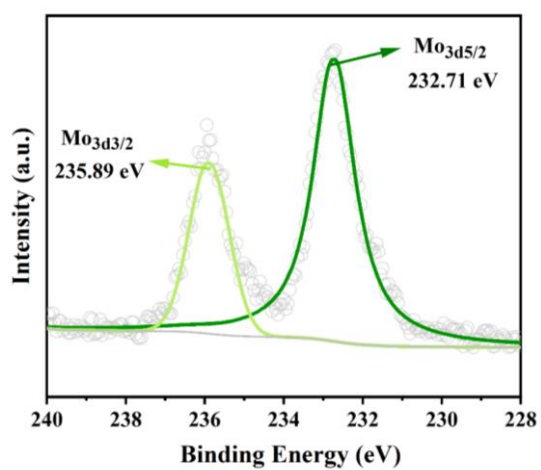


Figure S4. X-ray photoelectron spectra of PHGMo-15%.

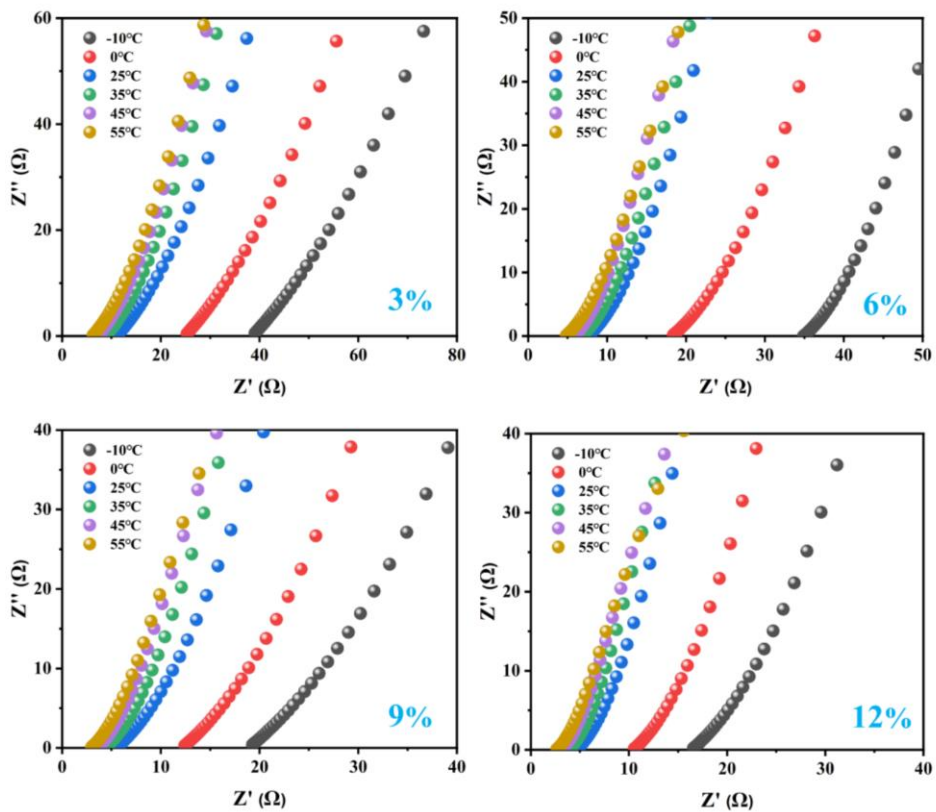


Figure S5. Nyquist plots of PHGMO- $x\%$ hydrogels ($x=3,6,9,12$).

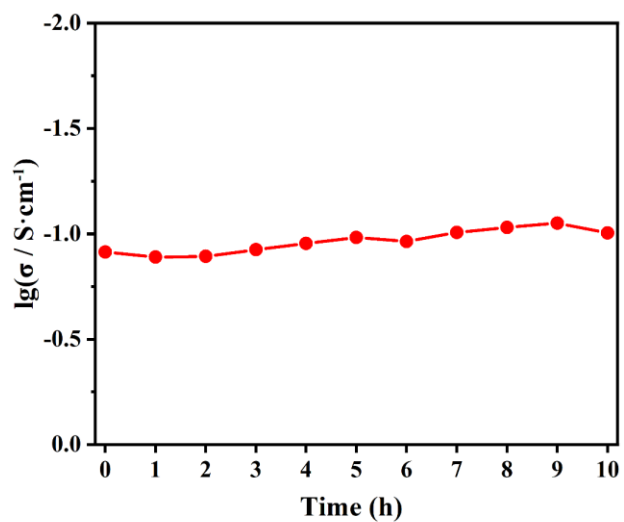


Figure S6. Long-term stability of the conductivity of PHGMO-15% hydrogel at room temperature.

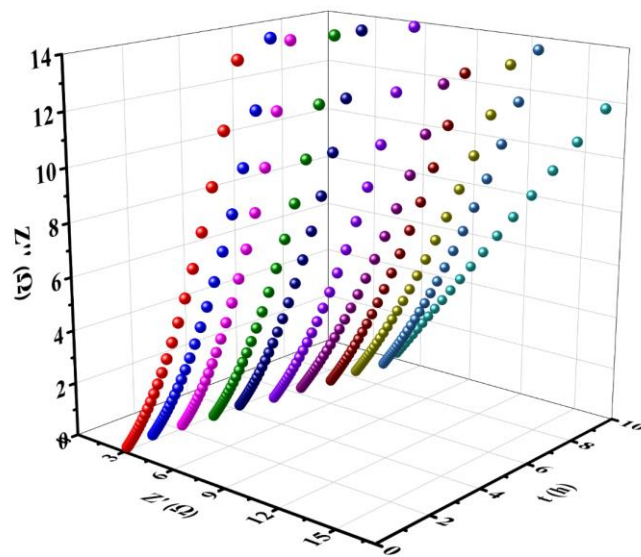


Figure S7. Nyquist plot of PHGMo-15% hydrogel at 25 °C with time.

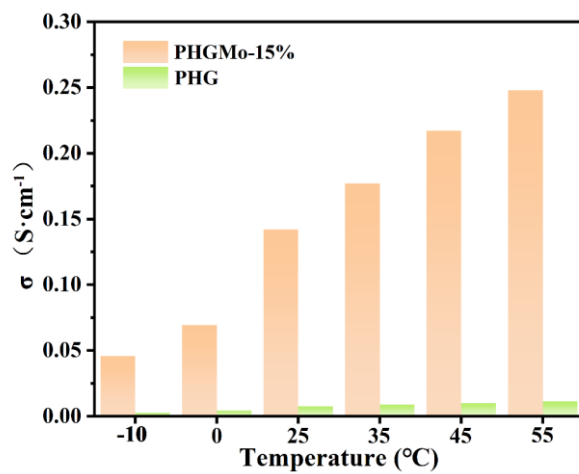


Figure S8. Comparison of conductivity of PHGMo-15% and PHG at -10-55°C.

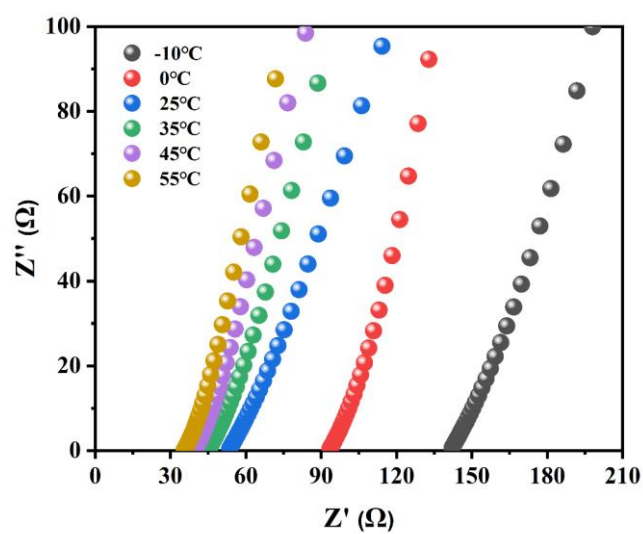


Figure S9. Nyquist plot of PHG hydrogel.

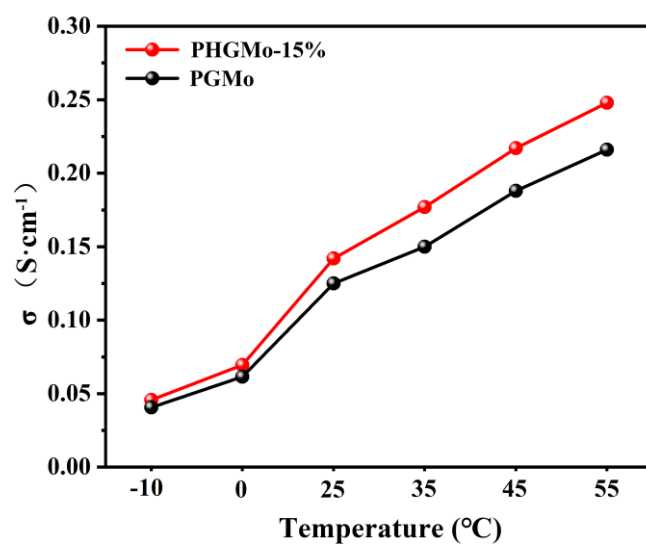


Figure S10. Comparison of conductivity of PHGMo-15% and PGMo at -10 - $55^{\circ}C$.

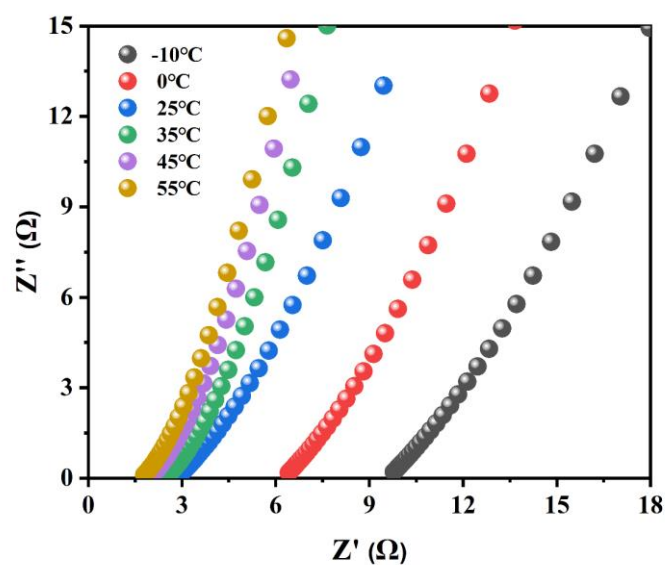


Figure S11. Nyquist plot of PGMo hydrogel.

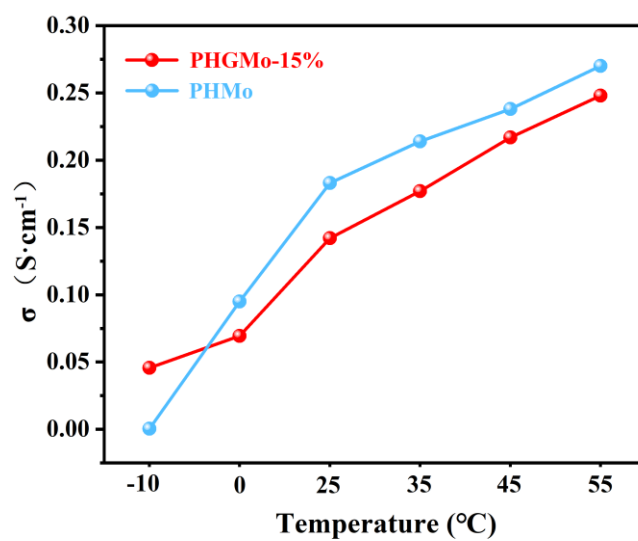


Figure S12. Comparison of conductivity of PHGMO-15% and PHMo at -10 - $55^{\circ}C$.

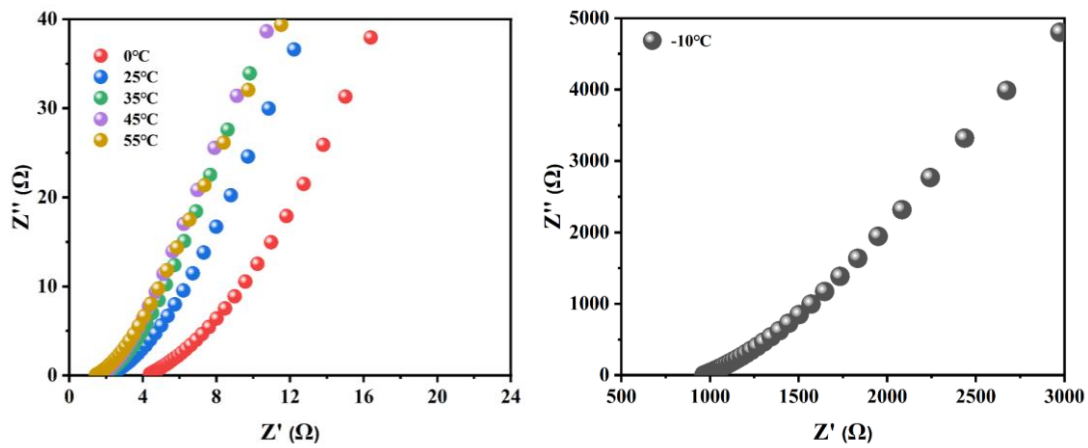


Figure S13. Nyquist plots of PHMo hydrogel.

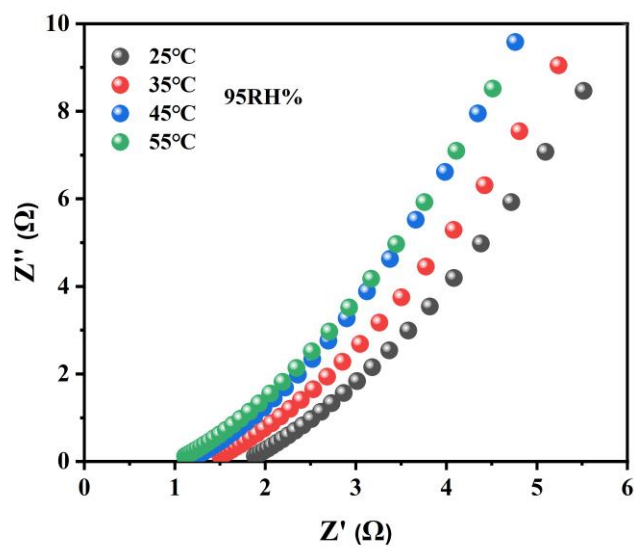


Figure S14. Nyquist plot of PHGMO-15% hydrogel at 95% RH and various temperatures.

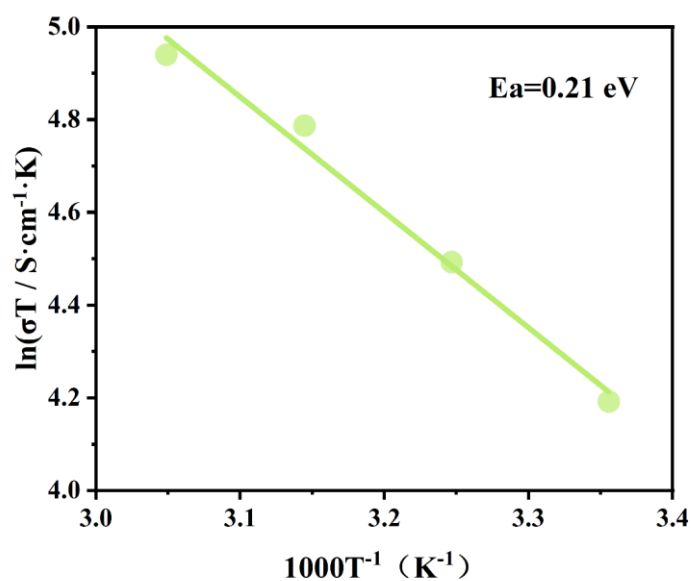


Figure S15. Arrhenius plot of the proton conductivity of PHGMo-15% hydrogel at 95% RH and various temperatures.

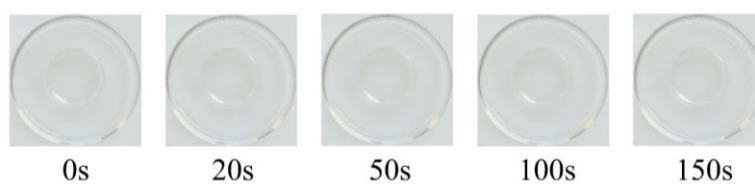


Figure S16. Pictures of PHG hydrogel under UV irradiation at different times.

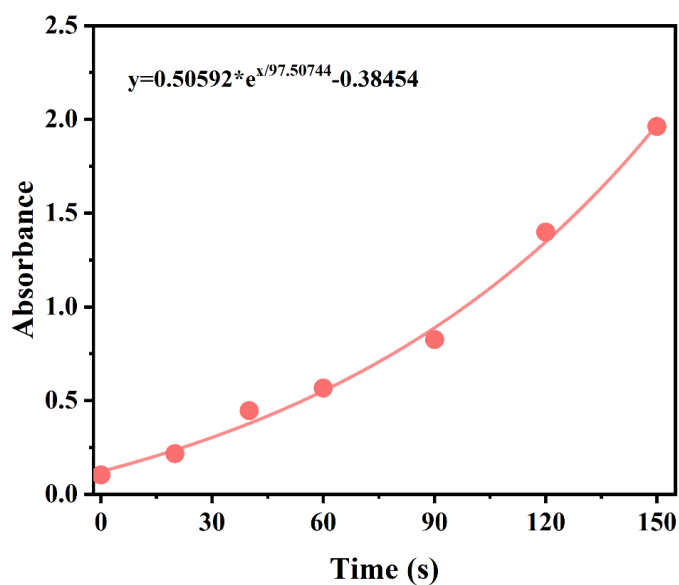


Figure S17. Fitted absorbance curve of PHGMo-15% at 740 nm under different UV irradiation times at room temperature.

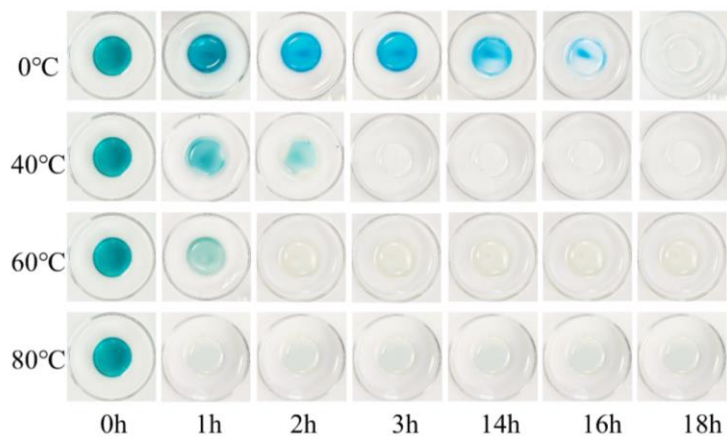


Figure S18. Color fading process of PHGMo-15% at different temperatures.

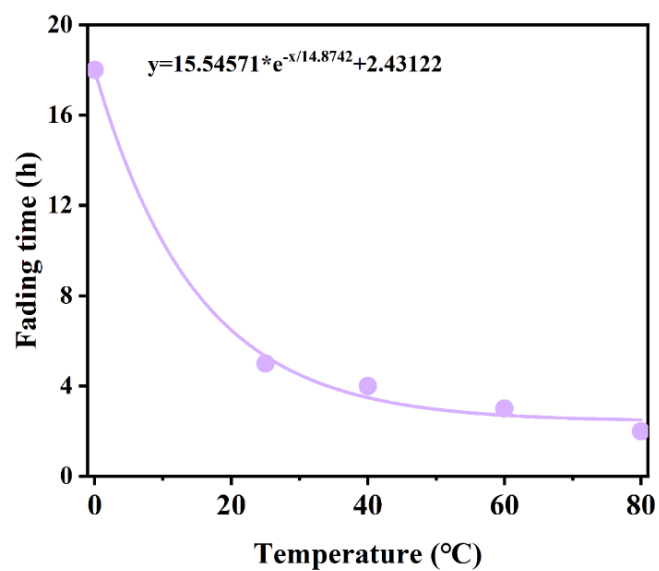


Figure S19. Fitting curve of fading time to absorbance at 740 nm for PHGMo-15% at different temperatures.

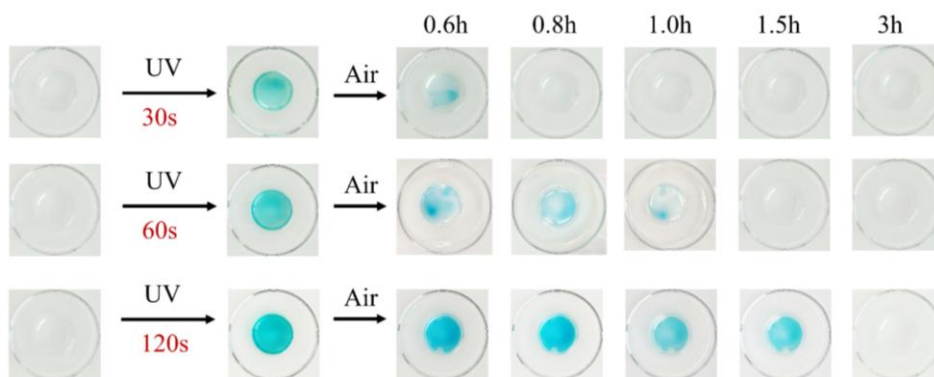


Figure S20. Color fading process of PHGMo-15% under different UV irradiation times.



Figure S21. Transparency of PHGMo-15% before and after the color change.

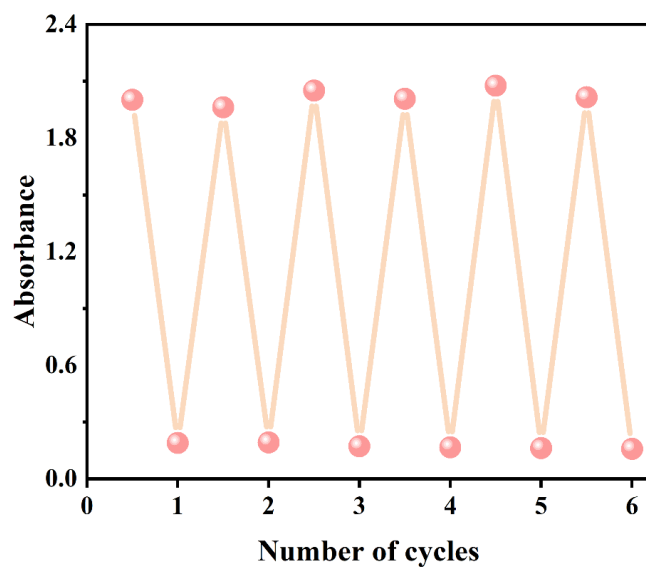


Figure S22. Absorbance at 740 nm of PHGMo-15% during photochromic and fading processes for more than 6 cycles.

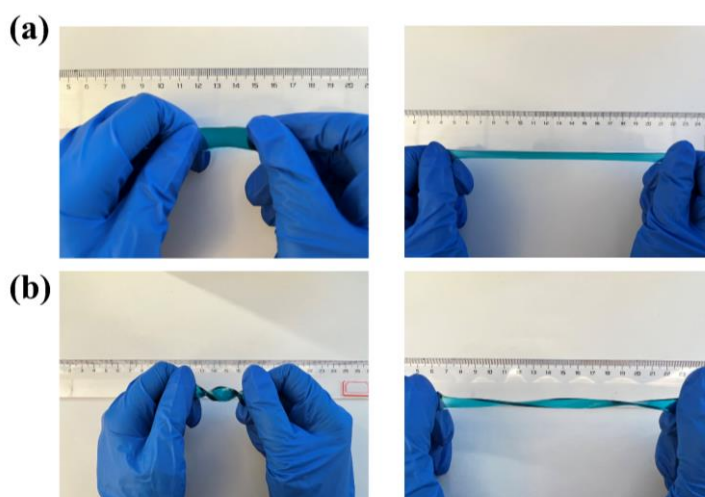


Figure S23. Photographs of PHGMo-15% hydrogel being stretched and twisted at room temperature.

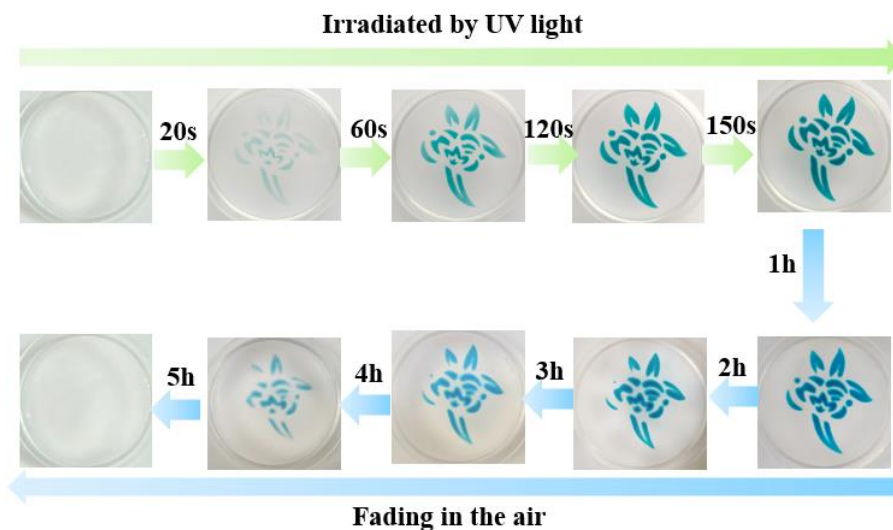


Figure S24. The process of PHGMO-15% of storing and erasing information at room temperature.

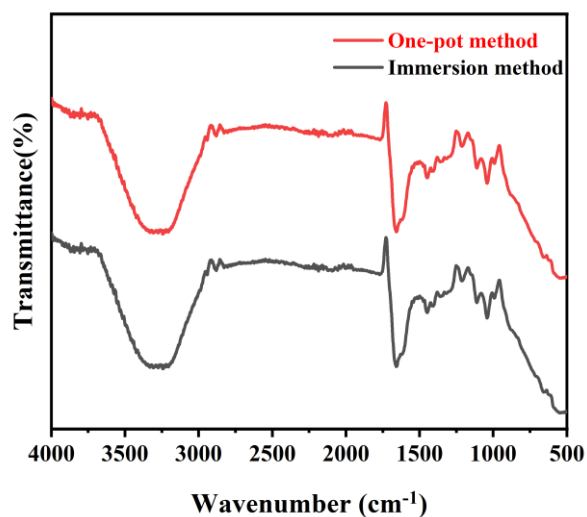


Figure S25. Comparison of the FTIR spectra of PHGMO-15% and PHG-15wt%-3h by different synthesis strategies

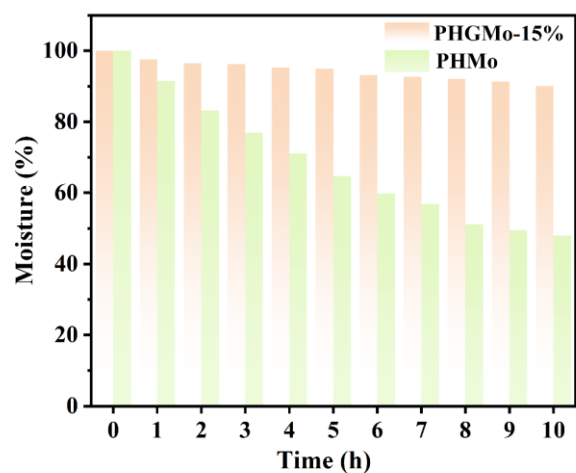


Figure S26. Water retention of PHGMo-15% hydrogel and PHMo hydrogel at room temperature and ambient humidity for 10 h.



Figure S27. Image of the state of human skin after 5 days of PHGMo-15% adhesion to human skin.

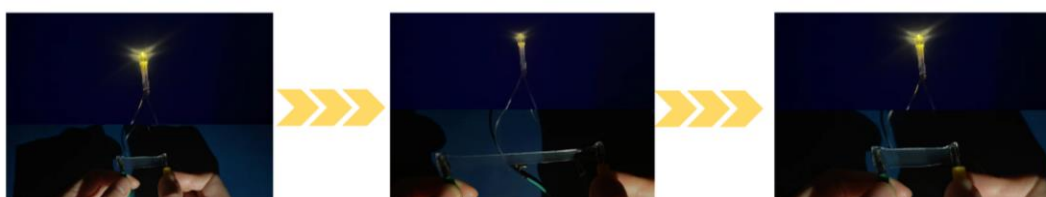


Figure S28. PHGMo-15% as a wire to light a small bulb during the stretching process.

Section 3: Supplementary Tables

Table S1. The ICP measurement of PHGMo-x% hydrogels and PHG hydrogel.

Samples	Elemental	Elemental Anal. /%
PHGMo-3%	Mo	2.26
PHGMo-6%	Mo	4.60
PHGMo-9%	Mo	6.74
PHGMo-12%	Mo	8.79
PHGMo-15%	Mo	10.76
PHG	Mo	0

Among them, the preparation process as well as the raw material additions of PHG hydrogel were consistent with PHGMo-x% hydrogels, except that Mo₇ was not added during the fabrication process.

Table S2. Comparison of the conductivity of conductive hydrogels with high conductivity at room temperature.

Hydrogel	Ionic conductivity (S·cm ⁻¹)	Ref.
PHGMo-15%	1.42×10⁻¹	This work
PC ₁ PAV ₃₀	1.52×10 ⁻²	1
PVA/CMC/CCNF-2M	3.5×10 ⁻²	2
pTPSS	8.2×10 ⁻⁴	3
AM4DMC1AA-Na/CNF-Cl	1.03×10 ⁻¹	4
PAMPS-K25-MC2.0-5M	1.05×10 ⁻¹	5
AAV-3	1.25×10 ⁻¹	6
OAL0.06-Fe0.6-PAA	2.57×10 ⁻²	7
PNMA/SA-0.3	3.31×10 ⁻²	8

PBLL	8.18×10^{-2}	9
Ion-CB	8.99×10^{-2}	10
PAM/CMC-2LiCl	3.651×10^{-2}	11
PVA-SiO ₂ -2/LiCl	5.617×10^{-2}	12
ICH-3	7.896×10^{-2}	13
PVA-SbQ/SA/FeCl ₃ /Gly	3.8×10^{-3}	14
PVA-CMC _{0.15} -LC _{0.15}	8.3×10^{-2}	15

Table S3. Proton conductivity of PHGMO-x% hydrogel at different temperatures ($S \cdot cm^{-1}$)

Temp ($^{\circ}C$)	x=3	x=6	x=9	x=12	x=15
55	6.35×10^{-2}	8.20×10^{-2}	1.30×10^{-1}	1.61×10^{-1}	2.48×10^{-1}
45	5.44×10^{-2}	6.99×10^{-2}	1.08×10^{-1}	1.25×10^{-1}	2.17×10^{-1}
35	4.49×10^{-2}	5.98×10^{-2}	8.93×10^{-2}	1.03×10^{-1}	1.77×10^{-1}
25	3.67×10^{-2}	5.16×10^{-2}	7.09×10^{-2}	8.53×10^{-2}	1.42×10^{-1}
0	1.58×10^{-2}	2.28×10^{-2}	3.28×10^{-2}	3.92×10^{-2}	6.94×10^{-2}
-10	1.03×10^{-2}	1.46×10^{-2}	2.11×10^{-2}	2.51×10^{-2}	4.57×10^{-2}

References

1. T. Lei, J. Pan, N. Wang, Z. Xia, Q. Zhang, J. Fan, L. Tao, W. Shou and Y. Gao, *Mater. Horiz.*, 2024, **11**, 1234-1250.
2. Q. Zhou, S. Lu, P. Xu, D. Niu, D. Puglia, W. Yang and P. Ma, *Green Chem.*, 2025, **27**, 684-695.
3. Q. Wang, H. Liu, M. Wang, H. Zhang, J. Xie, X. Hu, S. Zhou and W. Wu, *Chin. Chem. Lett.*, 2024, **35**, 108743.
4. R. Zhang, Z. Zhang, P. Xu, J. Xu, Y. Gao and G. Gao, *Carbohydr. Polym.*, 2024, **326**, 121654.
5. N. Sun, F. Lu, Y. Yu, L. Su, X. Gao and L. Zheng, *ACS Appl. Mater. Interfaces*, 2020, **12**, 11778-11788.
6. Y. Zhou, X. Fei, J. Tian, L. Xu and Y. Li, *J. Colloid Interface Sci.*, 2022, **606**, 192-203.
7. T. Song, Z. He, H. He, T. Wang, J. Du, Y. Lv, Y. Tao, J. Lu, C. Fu, J. Hu and H. Wang, *Chem.*

- Eng. J.*, 2024, **500**, 157220.
8. W. Zeng, S. Zhang, J. Lan, Y. Lv, G. Zhu, H. Huang, W. Lv and Y. Zhu, *ACS Nano*, 2024, **18**, 26391-26400.
 9. R. Liu, Y. Liu, S. Fu, Y. Cheng, K. Jin, J. Ma, Y. Wan and Y. Tian, *Small*, 2024, **20**, 2308092.
 10. S. Wang, L. Yu, S. Wang, L. Zhang, L. Chen, X. Xu, Z. Song, H. Liu and C. Chen, *Nat. Commun.*, 2022, **13**, 3408.
 11. W. Qian, S. Jia, P. Yu, K. Li, M. Li, J. Lan, Y. Lin and X. Yang, *Mater. Today Phys.*, 2024, **49**, 101589.
 12. C. Tang, Y. Yao, M. Li, Y. Wang, Y. Zhang, J. Zhu, L. Wang and L. Li, *Adv. Funct. Mater.*, 2024, 2417207.
 13. H. Miao, Y. Liu, C. Zheng, X. Huang, Y. Song, L. Tong, C. Dong, X. Fu, H. Huang, M. Ge, H. Liu and Y. Qian, *Carbohydr. Polym.*, 2025, **351**, 122936.
 14. D. Chen, H. Bai, H. Zhu, S. Zhang, W. Wang and W. Dong, *Chem. Eng. J.*, 2024, **480**, 148192.
 15. Y. Yang, K. Wang, Q. Zang, Q. Shi, Y. Wang, Z. Xiao, Q. Zhang and L. Wang, *J. Mater. Chem. A*, 2022, **10**, 11277-11287.